Developmental and Comparative Immunology 146 (2023) 104727

Contents lists available at ScienceDirect

Developmental and Comparative Immunology

journal homepage: www.elsevier.com/locate/devcompimm

DDX23 of black carp negatively regulates MAVS-mediated antiviral signaling in innate immune activation

Wei Qin [a], Yankai Liu [a], Jun Xiao [a,*], Nianfeng Chen [a], Jiagang Tu [b], Hui Wu [a], Yongan Zhang [b], Hao Feng [a,**]

[a] State Key Laboratory of Developmental Biology of Freshwater Fish, College of Life Science, Hunan Normal University, Changsha, 410081, China
[b] College of Fisheries, Huazhong Agricultural University, Wuhan, Hubei, 430070, China

ARTICLE INFO

Keywords:
Innate immunity
Black carp
IFN
DDX23
MAVS

ABSTRACT

Mammalian DDX23 is involved in multiple biological processes, such as RNA processing and antiviral responses. However, the function of teleost DDX23 still remains unclear. In this paper, we have cloned the DDX23 homologue of black carp (*Mylopharyngodon piceus*) (bcDDX23) and elucidated its role in the antiviral innate immunity. The coding region of bcDDX23 comprises 2427 nucleotides and encodes 809 amino acids. The transcription of bcDDX23 was promoted by the stimulation of LPS, poly(I:C), and SVCV; and immunoblotting (IB) assay showed that bcDDX23 migrated aground 94.5 kDa. Immunofluorescence (IF) assay revealed that bcDDX23 was mainly distributed in the nucleus, and the amount of cytosolic bcDDX23 was significantly increased after SVCV infection. The reporter assay showed that bcDDX23 inhibited bcMAVS-mediated transcription of the IFN promoter. And the co-immunoprecipitation (co-IP) assays identified the interaction between bcDDX23 and bcMAVS. Furthermore, co-expressed bcDDX23 significantly inhibited bcMAVS-mediated antiviral ability against SVCV in EPC cells, and knockdown of bcDDX23 enhanced the resistance of host cells against SVCV. Overall, our results conclude that bcDDX23 targets bcMAVS and suppresses MAVS-mediated IFN signaling, which sheds light on the regulation of IFN signaling in teleost fish.

1. Introduction

Vertebrates have evolved well-established immune systems, including innate immune system and adaptive immune system, that can effectively defend against the invasion of pathogenic microorganisms, suchlike bacteria and virus (Akira et al., 2006). However, adaptive immunity in lower vertebrates is less well developed compared to the higher vertebrates, so teleost fishes rely more on innate immunity to deal with potential threats (Zhu et al., 2013; Cao et al., 2021). The innate immune system recognizes conserved pathogen-associated molecular patterns (PAMPs) of pathogens through pattern recognition receptors (PRRs) and activates downstream signaling molecules that leads to antiviral immune responses (Carty et al., 2021; Takeuchi and Akira, 2010).

Retinoic acid-inducible gene-I (RIG-I) like receptors (RLRs) are the major PRRs that sense viral RNA. They consist of three members: RIG-I, melanoma differentiation-associated gene 5 (MDA5), and laboratory of genetic and physiology 2 (LGP2) (Fang et al., 2017). When viral RNA is detected, RIG-I and MDA5 interact through the N-terminal caspase recruitment structural domains (CARDs) with the CARD domain of the adapter protein mitochondrial antiviral signaling protein (MAVS), leading to the activation of MAVS. Activated MAVS then triggers a signaling cascade response that leads to activation and nuclear translocation of transcription factors interferon regulatory factors (IRFs) and nuclear factor κB (NF-κB), which induce IFN production and expression of pro-inflammatory cytokines (Ramos and Gale, 2011; Rehwinkel and Gack, 2020). MAVS-mediated antiviral signaling is strictly regulated to avoid excessive immune responses that may result in overproduction of IFN and self-damage (Funabiki et al., 2014; Rönnblom and Eloranta, 2013). Several negative regulators of MAVS have been identified in fish, such as NLRX1, RIPK1 and TRAFD1 in black carp and PIAS4a in zebrafish (Xiao et al., 2023). However, compared with mammals, our understanding about the regulation mechanism of MAVS in fish is not comprehensive.

* Corresponding author.
** Corresponding author.
E-mail addresses: xiaojun@hunnu.edu.cn (J. Xiao), fenghao@hunnu.edu.cn (H. Feng).

https://doi.org/10.1016/j.dci.2023.104727
Received 10 April 2023; Received in revised form 4 May 2023; Accepted 4 May 2023
Available online 9 May 2023

Table 1
Primers used in the study.

Primer	Sequence (5′-3′)	Application
bcDDX23-F	ATGGCTGGTGAGTCTTCTGATAAG	cloning of bcDDX23
bcDDX23-R	TCAAGCAAAGATGGTCTCCTCTC	
Expression construct		
bcDDX23-N-F	ACTGACGGTACCATGGCTGGTGAGTCTTC	pcDNA5/FRT/To-HA-bcDDX23
bcDDX23-N-R	ACTGACCTCGAGTCAAGCAAAGATGGTC	
q-PCR		
bc-actin-qF	TGGGCACCGCTGCTTCCT	*ex vivo* q-PCR
bc-actin-qR	TGTCCGTCAGGCAGCTCAT	
bcDDX23-qF	GCTGCTTGAGGTCGATGC	*ex vivo* q-PCR
bcDDX23-qR	TGGCGGAATGAAGAAACG	
EPC-actin-qF	AAGGAGAAGCTCTGCTATGTGGCT	*ex vivo* q-PCR
EPC-actin-qR	AAGGTGGTCTCATGGATACCGCAA	
EPC–IFN–qF	TGACTTGACCGAGTACAGC	*ex vivo* q-PCR
EPC–IFN–qR	ATGAAAACTCAAATGTGGACGTA	
EPC-IRF7-qF	GTGGGAAGTATGAGGGATTG	*ex vivo* q-PCR
EPC-IRF7-qR	TTCGCTTTGTCGTAAGGGTT	
EPC-MX1-qF	TGGAGGAACCTGCCTTAAATAC	*ex vivo* q-PCR
EPC-MX1-qR	GTCTTTGCTGTTGTCAGAAGATTAG	
EPC-PKR-qF	ACCTGAAGCCTCCAAACATA	*ex vivo* q-PCR
EPC-PKR-qR	GCATTCGCTCATCATTGTC	
bc-IFNa-qF	AAGGTGGAGGACCAGGTGAAGTTT	*ex vivo* q-PCR
bc-IFNa-qR	GACTCCTTATGTGATGGCTTGTGG	
bc-MX1-qF	TGAGCGTAGGCATTAGCAC	*ex vivo* q-PCR
bc-MX1-qR	CCTGGAGCAGCAGATAGCG	
bc-PKR-qF	GAGCGGACTAAAAGGACAGG	*ex vivo* q-PCR
bc-PKR-qR	AAAATATATGAGACCCAGGG	
bc-IRF7-qF	GTGGGCGGTATGAGGGATTG	*ex vivo* q-PCR
bc-IRF7-qR	TTGGCTTTGTCGTTAGGGTG	
SVCV-G-qF	GATGACTGGGAGTTAGATGGC	*ex vivo* q-PCR
SVCV-G-qR	ATGAGGGATAATATCGGCTTG	
SVCV-N-qF	GGTGCGAGTAGAAGACATCCCCG	*ex vivo* q-PCR
SVCV-N-qR	GTAATTCCCATCATTGCCCCAGAC	
SVCV-M-qF	CGACCGCGCCAGTATTGATGGATAC	*ex vivo* q-PCR
SVCV-M-qR	ACAAGGCCGACCCGTCAACAGAG	
SVCV-P-qF	AACAGGTATCGACTATGGAAGAGC	*ex vivo* q-PCR
SVCV-P-qR	GATTCCTCTTCCCAATTGACTGTC	
Knockdown		
sh bcDDX23-1-F	CCGGGGATGGAAAGAGAGAACAATGCTCGAGCATTGTTCTCTCTTTCCATCCTTTTTG	shRNA
sh bcDDX23-1-R	AATTCAAAAAGGATGGAAAGAGAGAACAATGCTCGAGCATTGTTCTCTCTTTCCATCC	
sh bcDDX23-2-F	CCGGGCCTATCATCATCTTCGTTAACTCGAGTTAACGAAGATGATGATAGGCTTTTTG	shRNA
sh bcDDX23-2-R	AATTCAAAAAGCCTATCATCATCTTCGTTAACTCGAGTTAACGAAGATGATGATAGGC	

As family members of RNA helicases, DEAD/H-box proteins have been reported to involve in many aspects of RNA metabolism, for instance RNA transcription, pre-mRNA alternative splicing and RNA translocation etc. (Konishi et al., 2008; Krishnan and Zeichner, 2004). DEAD-box helicase 23 (DDX23) was first isolated from *Saccharomyces cerevisiae* and originally called Prp28p (Abdullah et al., 2020; Chen et al., 2001). Recent studies on the antiviral functions of DDX23 have increased, such as the over-expression of DDX23 can reduce the replication of Foot-and-Mouth Disease Virus (FMDV) in infected cells and DDX23 knockdown significantly reduces secretion of interferon-stimulated genes in vesicular stomatitis virus (VSV)-infected cells (Abdullah et al., 2020; Ruan et al., 2019). DDX23 has also been identified as an emerging PRR that is able to sense dsRNA. When stimulated by VSV, human DDX23 is capable of translocating from the nucleus to the cytoplasm and binding to TRIF or MAVS, which in turn activates the IFN-induced antiviral immune response (Bonaventure and Goujon, 2022; Ruan et al., 2019). However, poorly known is how DDX23 works in the innate antiviral immune response in fish.

Black carp is an economically important fish in China with yearly output over 700,000 tons, which ranks eighth among all freshwater fish production. However, its aquaculture industry is severely threatened by a bulk of pathogenic microbes, suchlike Spring Viremia of Carp Virus (SVCV) (Ashraf et al., 2016; Liu et al., 2022). Currently, fish diseases have gradually become one of the bottlenecks limiting the sustainable development of the black carp farming industry. Therefore, the study of antiviral innate immunity in black carp is of great significance. In this study, we have cloned and identified black carp DDX23, which is able to interact with bcMAVS, thereby inhibiting antiviral signaling and leading to diminished antiviral activity in host cells. To our knowledge, this study demonstrates for the first time in fish that bcDDX23 is a negative regulator of antiviral innate immunity.

2. Materials and methods

2.1. Cells, virus, plasmids and transfection

HEK293T cells were original from ATCC and kept in the lab. *Epithelioma papulosum cyprinid* (EPC) cells and *Mylopharyngodon piceus* kindey (MPK) cells were presented as gifts from Dr. Jianguo Su and Dr. Tiansheng Chen (Huazhong Agricultural University) respectively and kept in lab (Xue et al., 2018). All these cells were cultured following the methods introduced in the reference (Wang et al., 2021).

SVCV (strain: SVCV 741) was kept in the lab. The SVCV used in this study is the same virus batch as mentioned in our previously study. The virus reproduction and titers detection were conducted as mentioned previously (Liu et al., 2022). In short, EPC cells were infected with serial 10-fold gradient dilutions of virus, incubated at 26 °C for 2 h and the supernatant was substituted with fresh DMEM containing 2% FBS and 1% methylcellulose, and plaques were counted 3 days post infection. Virus titers were calculated using three groups of parallel data. In this paper, the titer of SVCV was 1.5×10^7 pfu/mL.

pcDNA5/FRT/TO, pcDNA5/FRT/TO-Flag-bcMAVS, PLKO.1-TRC, pRL-TK, the three types of type-I IFNs, Luci-DrIFNφ1 (for analyzing the activity of zebrafish IFNφ1 promoter), Luci-bcIFNa (for analyzing the

activity of black carp IFNa promoter) and Luci-eIFN (for analyzing the activity of the EPC IFN promoter) were kept in the lab (Yang et al., 2023). For HEK293T cells and EPC cells, polyetherimide (PEI) (Polysciences, USA) was applied for transfection. For MPK cells, LipoMax (SUDGEN, China) were used to increase the transfection efficiency. Transfection was performed according to the previous method (Wang et al., 2021). In brief, the cells were seeded the day before transfection and changed fresh media 0.5 h before adding the transfection mixture. Then plasmids and PEI/LipoMax were diluted with DMEM and mixed. Following, the mixture was deposited at room temperature for 15 min before adding to the cells. Finally, the mixture was replaced with fresh media 6 h after transfection.

2.2. Cloning the CDS of bcDDX23

The cDNA template used for cloning the CDS of bcDDX23 was obtained as described in previous paper (Liu et al., 2022). The primers bcDDX23-F/R were designed referencing to the predicted sequence of bcDDX23 in full-length transcriptome of black carp (unpublished data) (Table 1). The PCR program for amplifying the CDS of bcDDX23 performed as follows: 94 °C/5min; 32 cycles, 94 °C/30s, 55 °C/30s, 72 °C/2min30s; 72 °C/7min. The amplification products were inserted into pMD-18-T vectors and then sequenced by TSINGKE (Changsha, China). The recombinant plasmid pMD18-T/bcDDX23 was used as template to constructed the expressing vectors using the primers bcDDX23-N-F: ACTGACGGTACCATGGCTGGTGAGTCTTC and bcDDX23-N-R: ACTGACC- TCGAGTCAAGCAAAGATGGTC (Table 1). The amplified bcDDX23 CDS sequences by the primers bcDDX23-N-F/R were digested with *Kpn*I and *Xho*I to form the nick ends. And then ligated by T4 ligase with pcDNA5/FRT/TO vector, which expresses HA tag. The bcDDX23 expression vector was sequenced to confirm the correct fusing expression with the tag protein.

2.3. Sequence and phylogenetic analysis

Multiple sequence alignment of bcDDX23 with its homologous gene from other vertebrates was performed by using MEGAX software. The bcDDX23 secondary structure was predicted by the SWISS-MODEL online tool (https://www.swissmodel.expasy.org/). The results were edited using the ESPript 3.0 (https://espript.ibcp.fr/ESPript/cgi-bin/ESPript.cgi) program. Briefly, the FASTA file obtained by sequence alignment with MAGAX software and the PDB file obtained by SWISS-MODLE predicting the three-dimensional structure of bcDDX23 protein were imported into ESPript 3.0, and the parameters were set according to the operation instructions (Robert and Gouet, 2014). The molecular weight (Mw) of bcDDX23 was predicted by using the website EXPASy (https://web.expasy. org/compute_pi/). The DDX23 protein sequences of all species selected for the construction of the phylogenetic tree are placed in a FASTA format file. All these DDX23 protein sequences were aligned by MEGAX software. And the neighbor-joining method were selected to construct the phylogenetic tree. The protein domains were predicted by using the online tool SMART (http://smart.emble-heidelberg.de). Protein three-dimensional structure of bcDDX23 and human DDX23 (hDDX23) was predicted by the SWISS-MODEL online tool.

2.4. Quantitative real-time PCR

For the experiments to exam bcDDX23 gene expression in response to different stimuli in vitro, qPCR was used to measure the mRNA expression levels of bcDDX23 in MPK cells after 1 μg/mL and 5 μg/mL LPS, 5 μg/mL and 50 μg/mL Poly (I:C) stimulation and different MOI of SVCV (0.1 and 0.01) infection respectively. For the experiments to test the influence of over-expression of bcDDX23 in bcMAVS-mediated antiviral response, EPC cells in 6-well plate were co-transfected with bcDDX23 and bcMAVS. The mRNA expression levels of RLR/IFN signaling after SVCV infection, such as *epcIFN, epcMX1*, *epcPKR* and *epcIRF7,* and the virus genes suchlike *SVCV-G*, *N*, *M* and *P* were examined by qPCR. For the experiments to investigate the affect of knockdown bcDDX23 in host antiviral signaling, the mRNA expression levels of host antiviral genes such as *bcIFNa*, *bcMX1*, *bcPKR* and *bcIRF7* and virus genes *SVCV-G*, *N*, *M* and *P*, were detected by qPCR 24 h after SVCV infection. The primers used in qPCR were appended in Table 1. For qPCR assays, total RNA was isolated from the treated EPC or MPK cells. Then, cDNA were synthesized following the instructions of the cDNA synthesis kit (Takara). The SYBR Green detection system (Invitrogen) was utilized for qPCR, and the program was same as used in previous paper (Chen et al., 2021). The qPCR data were analyzed using the $2^{-\Delta\Delta}$CT relative quantification method, and the fold change between the experimental group and the control group represents the relative expression of the target gene.

2.5. bcDDX23 protein expression in vitro

The protein expression of bcDDX23 in vitro was conducted both in mammalian and fish cells by immunoblotting (IB). HEK293T and EPC cells were cultured in 6-well plates and subsequently transfected with empty vector and pcDNA5/FRT/TO-HA-bcDDX23, separately. The exogenous expression of bcDDX23 was examined 48 h after transfection. For detecting the knockdown effect of bcDDX23, HEK293T cells were seeded in 6-well plates and subsequently co-transfected with plasmids expressing bcDDX23 with shDDX23 or Scramble shRNA, respectively. The expression level of bcDDX23 was then detected by IB assay. Cell transfection and IB were performed as described previously (Yang et al., 2023).

2.6. Luciferase reporter assay

To investigate the effect of bcDDX23 on the transcriptional activity of the IFN promoter, EPC cells were cultured in 24-well plates and then the reporter plasmids pRL-TK, Luci-bcIFNa (Luci-eIFNa or Luci-DrIFNφ1) were co-transfected with pcDNA5/FRT/TO/HA-bcDDX23 or/and poly(I:C) into EPC cells. For studying the influence of bcDDX23 on bcMAVS-mediated IFN promoter transcriptional activity, the indicated plasmids were co-transfected in 24-well plates as described. The empty vectors were used in order to assure that the total amount of DNA was equal for each transfection. The cells were harvested 24 h after transfection and used for luciferase activity assay according to the instructions of the Reporter Assay System kit (Promega, USA). The detailed operation was mentioned in our previous paper (Chen et al., 2021).

2.7. Immunofluorescence

To detect the subcellular localization of bcDDX23 before and after viral infection, pcDNA5/FRT/TO-HA-bcDDX23 was transfected into EPC cells and immunofluorescence detection was performed. The sample preparation method was same as described in a previous paper (Liu et al., 2022). Briefly, the cells were fixed with 4% paraformaldehyde and then permeabilized with 0.2% Triton X-100 and blocked with 10% FBS, washed with PBS. Next, the cells were incubated with rabbit monoclonal anti-HA antibody (1:500), washed with PBS, and then probed with secondary antibody Alexa 488 conjugated anti-rabbit antibody at the ration of 1:1000. 8 μL DAPI (Sigma) were used for stained with the cells before sealing the coverslips. Laser scanning confocal microscope (Olympus FV1200, Japan) was used to capture the image.

2.8. Virus infection

To detect the anti-SVCV ability of EPC cells over-expressing bcDDX23, cells were seeded in 24-well plates 16–24 h before transfection, and then transfected with the plasmids expressing bcDDX23,

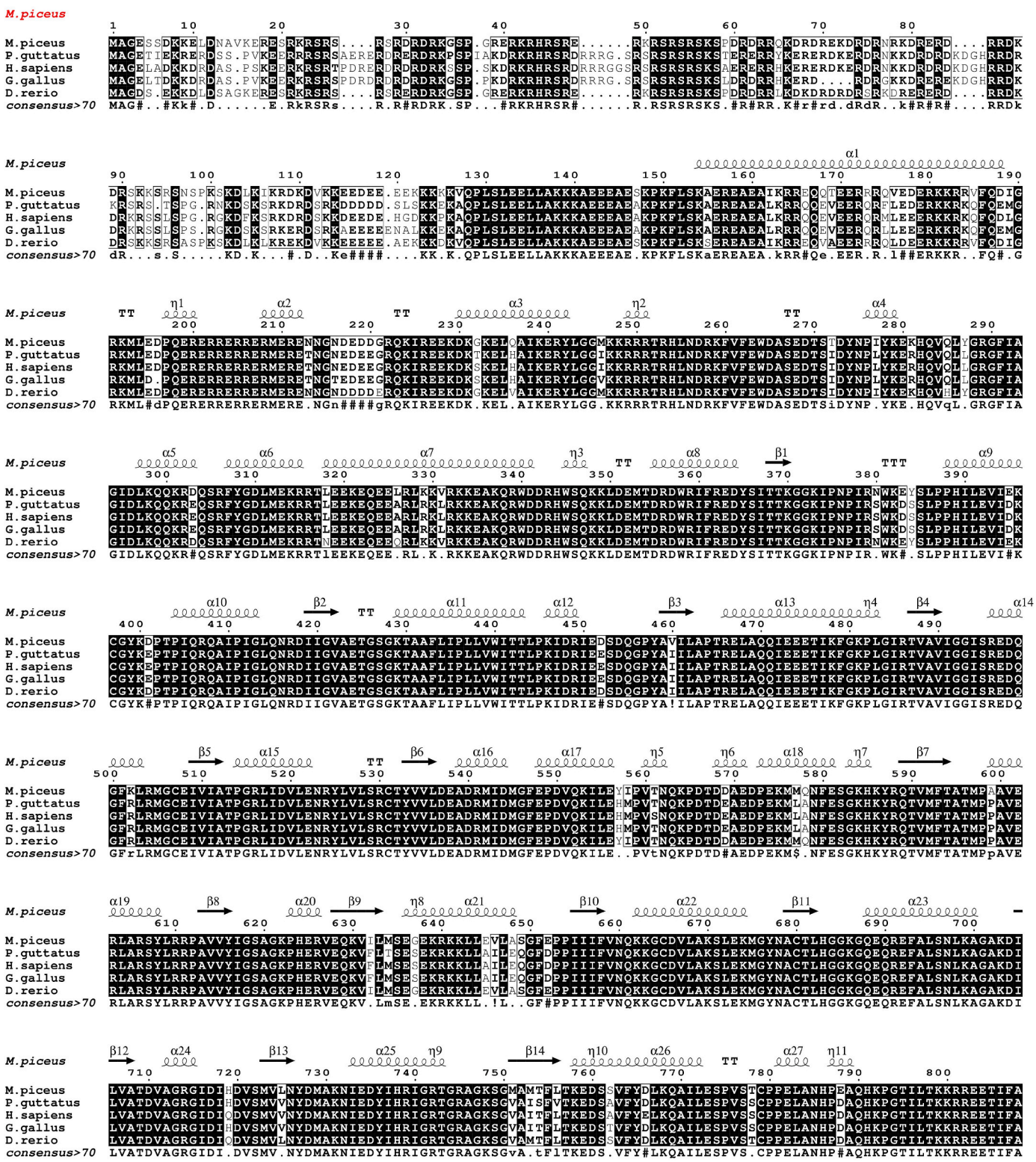

Fig. 1. Multiple alignments of DDX23.
Multisequence alignment of DDX23 from *Mylopharyngodon piceus* (OQ725692), *Homo sapiens* (NP_004809.2), *Danio rerio* (NP_956176.1), *Pantherophis guttatus* (XP_034268200.1), *Gallus gallus* (XP_025001442.1). α, β and η represent α-helices, β-sheets and 3_{10}-helices respectively, strict α-turns are indicated with TTT, strict β-turns with TT.

bcMAVS or empty vectors. 24 h post transfection (hpt), cells were challenged with SVCV at the indicated MOI. After incubation for 1 h, the medium containing SVCV was removed. Then the cells were washed twice with DMEM, and added with fresh low serum culture medium (2% FBS). 24 h post infection, the supernatant was gathered for virus titer detection, using the method introduced in section 2.1. Each viral titer experiment was carried out in triplicates. To detect the impact of knocking down bcDDX23 in host antiviral ability, MPK cells were seeded

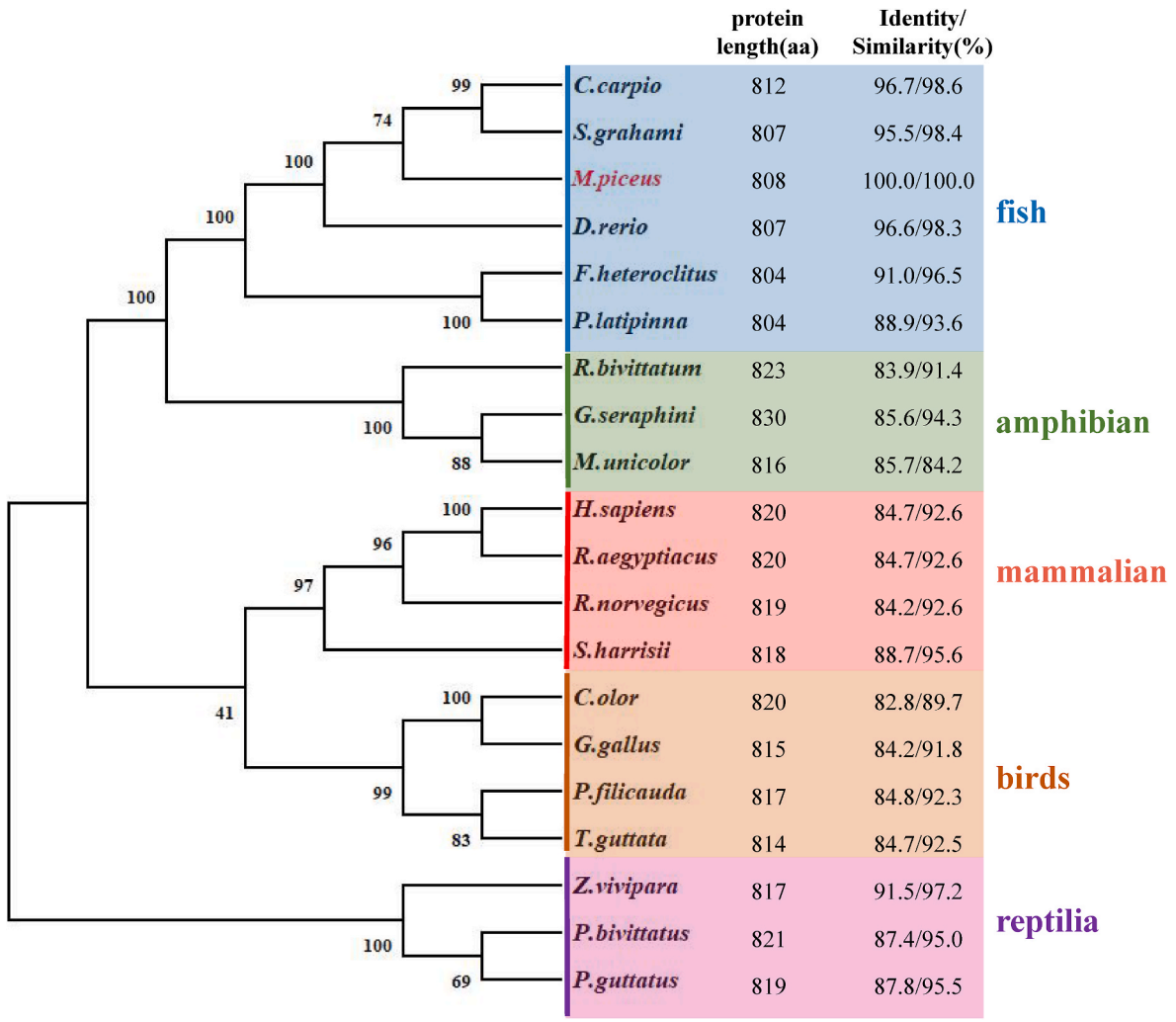

Fig. 2. Evolution of vertebrate DDX23.
The Phylogenetic trees were generated from different species of vertebrate DDX23, including: *Mylopharyngodon piceus* (OQ725692), *Homo sapiens* (NP_004809.2), *Danio rerio* (NP_956176.1), *Pantherophis guttatus* (XP_034268200.1), *Gallus gallus* (XP_025001442.1), *Cygnus olor* (XP_040395635.1), *Rhinatrema bivittatum* (XP_029450491.1), *Fundulus heteroclitus* (XP_012721390.2), *Microcaecilia unicolor* (XP_030052686.1), *Pipra filicauda* (XP_027587668.1), *Poecilia latipinna* (XP_014910666.1), *Rousettus aegyptiacus* (XP_016007229.1), *Python bivittatus* (XP_025026391.1), *Rattus norvegicus* (NP_001100263.2), *Sarcophilus harrisii* (XP_003766366.1), *Sinocyclocheilus graham* (XP_016139527.1), *Taeniopygia guttata* (XP_030115196.1), *Cyprinus carpio* (XP_042606114.1), *Zootoca vivipara* (XP_034956965.1), *Geotrypetes seraphini* (XP_033793739.1).

in 6 or 24-well plates, and transfected with bcDDX23 shRNA plasmids or nonsense control shRNA plasmids. The virus infection and titer detection methods were conducted as mentioned above. To assay the ability of EPC cells over-expressing bcDDX23 to resist SVCV invasion, different from the above steps, after washing twice with DMEM, semisolid culture medium supplemented with 1% methylcellulose was added instead of low serum culture medium. The cells were incubated in the semisolid culture medium for 48 h and then stained with crystal violet. The staining method was described as in the reference (Liu et al., 2022). Briefly, after 48 h of infection the supernatant was removed and the cell monolayer was washed once with PBS, then fixed with 10% methanol, washed once with PBS, and finally stained with crystal violet.

2.9. DDX23 shRNA design

To construct bcDDX23 shRNA oligonucleotides, the online tool GPP Web Portal (https://portals.broadinstitute.org/gpp/public/seq/search) was utilized. The bcDDX23 shRNA primers (Table 1) were synthesized by TSINGKE. The bcDDX23 shRNA plasmids, including PLKO-shRNA-bcDDX23-1 and PLKO-shRNA-bcDDX23-2, were obtained by inserting the target fragments into the PLKO.1-TRC plasmids.

2.10. Co-immunoprecipitation (co-IP) assay between bcDDX23 and bcMAVS

HEK293T cells seeding in 10 cm dishes were transfected with plasmids expressing bcDDX23 with/without bcMAVS. The transfected cells were collected for sample preparation 48 hpt. In brief, cells were lysed in NP40 buffer with cocktail protease inhibitor. Then the whole cell lysate (WCL) was incubated with protein A/G agarose beads at 4 °C for 2 h for precleaning. After that, anti-Flag (or anti-HA) agarose beads were added the WCL to precipitate the corresponding protein. The coprecipitated protein was then dissociated by boiling and sampled for IB analysis. The IB method was described as in the reference (Liu et al., 2022).

2.11. Statistics analysis

In present study, all data for the statistical analysis were collected from three separate experiments, each conducted in triplicate. The standard error of the mean value (+SEM) from three separate studies

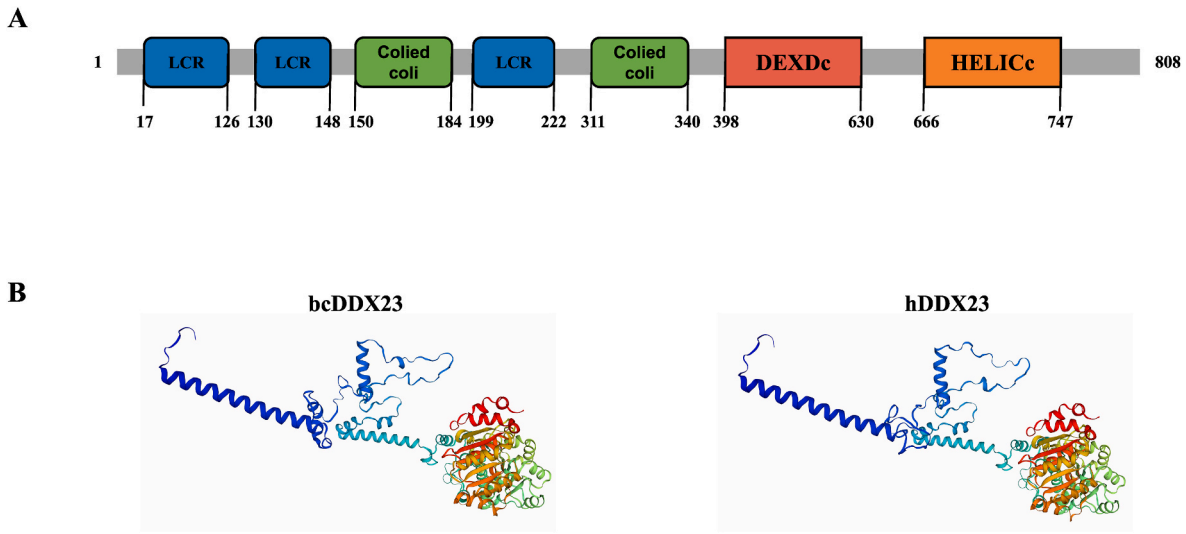

Fig. 3. Structural analysis of bcDDX23.
(**A**) The structure of bcDDX23 predicted by SMART program. LCR: low complexity region, Coiled coil: coiled coil region, DEXDc: DEAD-like helicase superfamily domain, HELICc: helicase superfamily c-terminal domain. (**B**): The three-dimensional protein structures of bcDDX23 and human DDX23 (hDDX23) predicted by the online tool SWISS-MODEL.

was represented by error bars. The pillar's asterisks (*) indicated that there was a significant difference between the two groups data (ns: no significance; *p < 0.05; **<p 0.01). Two-tailed Student's t-test was used to compare the data between the two groups.

3. Results

3.1. Sequence analysis of bcDDX23

To investigate the function of DDX23 in fish, the bcDDX23 was cloned and the plasmid expressing bcDDX23 was constructed. The results showed that bcDDX23 comprised 2427 nucleotides, encoding 809 amino acids (Fig. 1). By aligning bcDDX23 with the homologous protein sequences from other vertebrates (*Danio rerio*、*Pantherophis guttatus*、*Gallus gallus*、*Homo sapiens*), the results showed that amino acid sequences of DDX23 were highly conserved in different vertebrates, except in its N-terminal region, which were variable across vertebrates (Fig. 1). To investigate the evolution of DDX23 in vertebrates, a phylogenetic tree was constructed using DDX23 from different vertebrates, which included fish, amphibians, reptiles, birds and mammals. By analyzing the homology of the selected species and phylogenetic tree, the results showed that bcDDX23 possessed a high similarity and identity with DDX23 of other vertebrates, and bcDDX23 clustered with DDX23 of other fishes as a monophyletic group (Fig. 2). The structure analysis showed that bcDDX23 consisted of an N-terminal region, the DEAD-like helicases superfamily domain (DEXDc) and the helicase superfamily c-terminal domain (HELICc), whose N-terminal region contains three low-complexity regions (LCR) and two coiled-coil regions (Fig. 3A). The predicted three-dimensional structures between bcDDX23 and hDDX23 proteins showed high similarity, which was consistent with the results of sequence alignment (Fig. 3B). In conclusion, these results suggest evolutionary conservation of the main structural component of bcDDX23.

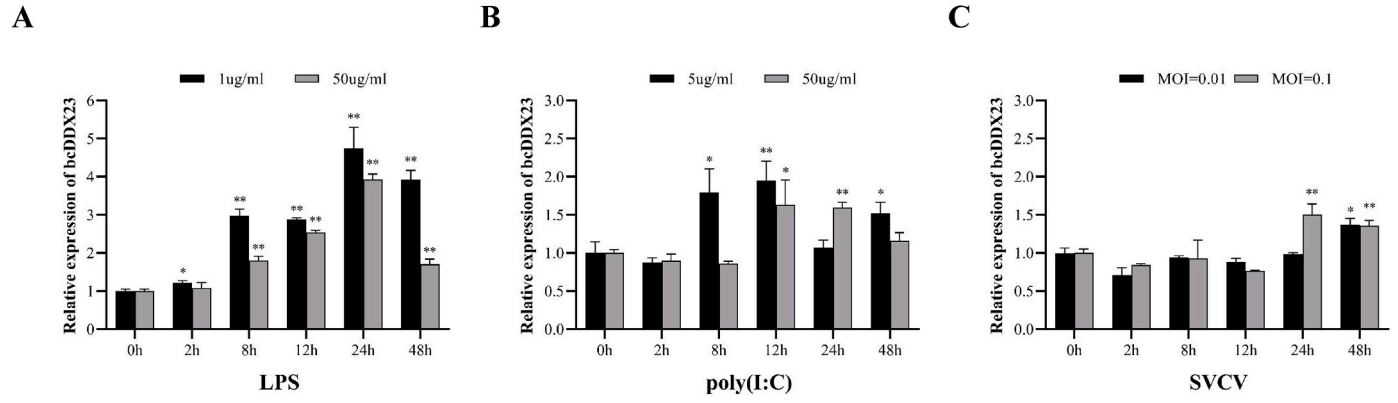

Fig. 4. bcDDX23 is involved in the host's innate immune response.
(**A-C**): MPK cells were seeded in 6-well plates (2×10^6 cells/well) and cells were treated with LPS or poly(I:C) or infected with SVCV. The quantification analysis of mRNA levels of bcDDX23 under different stimuli by qPCR. The mRNA levels of bcDDX23 in MPK cells at different time points after stimulation with different concentrations of LPS (A). Expression profile of bcDDX23 in MPK cells at different time points after Poly (I:C) treatment for indicated dosage (B). Expression profile of bcDDX23 in MPK cells at different time points post SVCV infection with the indicated MOI (C). Statistical analysis was conducted using the 0 h group as the control in each treatment. The number above the error bar represents the average bcDDX23 mRNA level. The asterisk (* or **) represents the fold changes are significant different compared with the 0 h group. *p < 0.05, **p < 0.01.

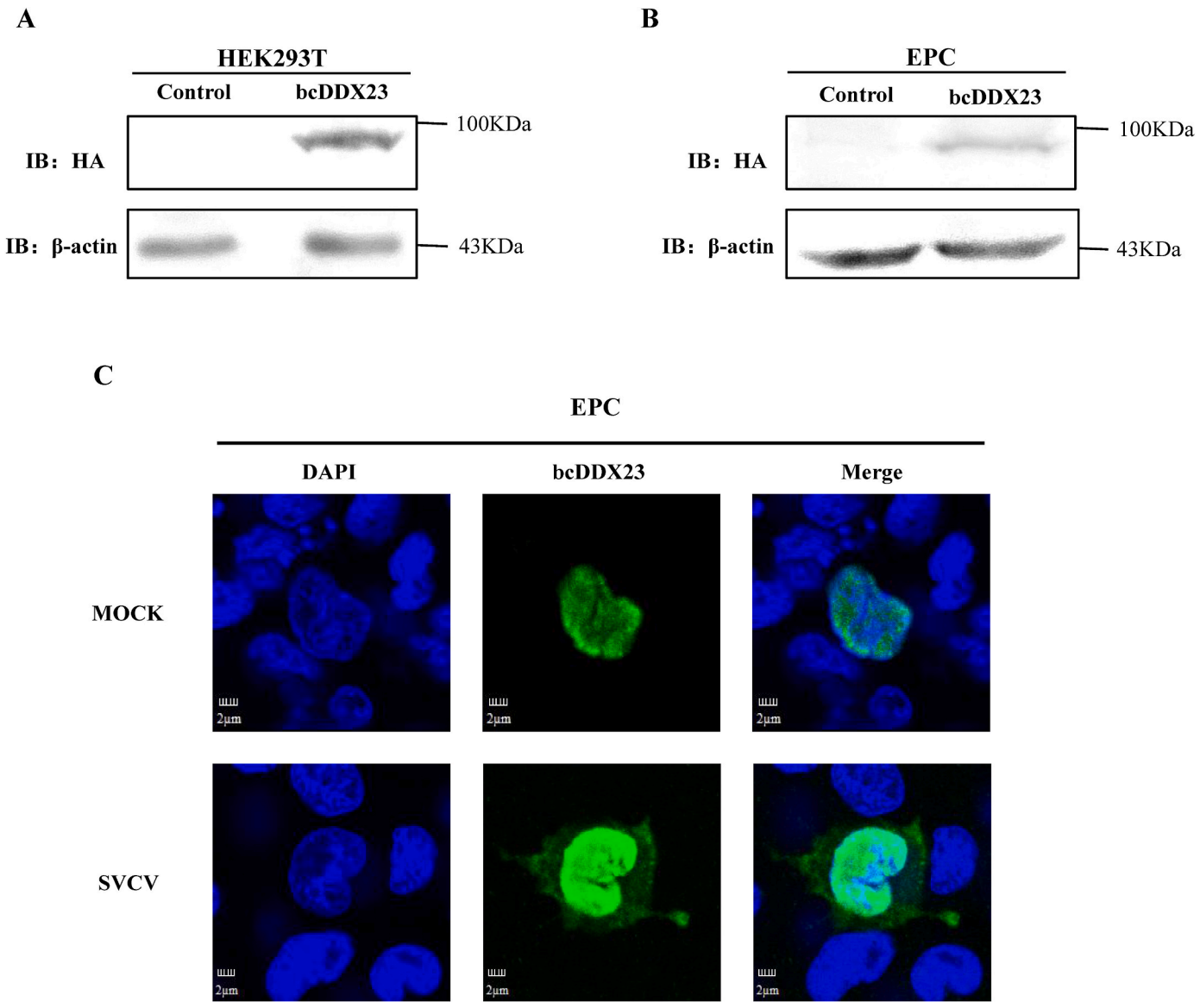

Fig. 5. The protein expression and subcellular localization of bcDDX23.
(**A-B**): HEK293T cells (A) or EPC cells (B) were transfected with bcDDX23, or empty vector (3 μg/well), and the expression of bcDDX23 was detected by immunoblotting (IB). (**C**): EPC cells were transfected with bcDDX23 and infected with or without SVCV at the MOI of 0.1 for 8 h. Cells were probe with anti-HA antibody and stained with DAPI and imaged using a confocal laser scanning microscope. bcDDX23: pcDNA5/FRT/TO/HA-bcDDX23; control: pcDNA5/FRT/TO; MOCK: cells not infected with SVCV; SVCV: cells infected with SVCV. The bars stand for the scale of 2 μm as showed in the pictures.

3.2. bcDDX23 is involved in the host's innate immune response

The mRNA expression of bcDDX23 respond to LPS, poly (I:C) treatment and SVCV infection were investigated in this research. The results showed that after LPS stimulation, the expression level of bcDDX23 mRNA was already up-regulated at 2 h in both the high (50 μg/mL) and low (1 μg/mL) dose treatment groups, and gradually increased with time, reaching the highest level at 12 h (Fig. 4A). This indicates that bcDDX23 may be involved in antimicrobial immune response. After poly (I:C) treatment, there was an up-regulation of bcDDX23 mRNA transcripts in the 5 μg/mL treated group at 8 h and reached the maximum fold change at 12 h (Fig. 4B). When infected with SVCV, there was an increase in the expression level of bcDDX23 at 24 hpi. At MOI = 0.1 and MOI = 0.01, the expression level of bcDDX23 had the highest fold change at 24 and 48 h, respectively (Fig. 4C). In conclusion, these data hint that bcDDX23 is probability involved in the black carp antiviral immune response.

3.3. The protein expression and subcellular location of bcDDX23

According to the prediction results of ExPASY, the molecular weight of bcDDX23 was expected to be 94.5 kDa. The protein expression level of bcDDX23 in HEK293T cells and EPC cells were detected through IB assay (Fig. 5A–B). A specific band of slightly less than 100 kDa was detected in the lane representing cells over-expressing bcDDX23, while no corresponding specific band was detected in the control. This indicates that bcDDX23 expressing vector can be correctly expressed both in mammalian and fish cells. Subsequent immunofluorescence experiments showed that bcDDX23 (green signal) was mainly located in the nucleus and that the distribution of bcDDX23 in the cytoplasm increased remarkably after SVCV stimulation (Fig. 5C). This suggests that bcDDX23 is a nuclear protein that translocates to the cytoplasm after SVCV stimulation.

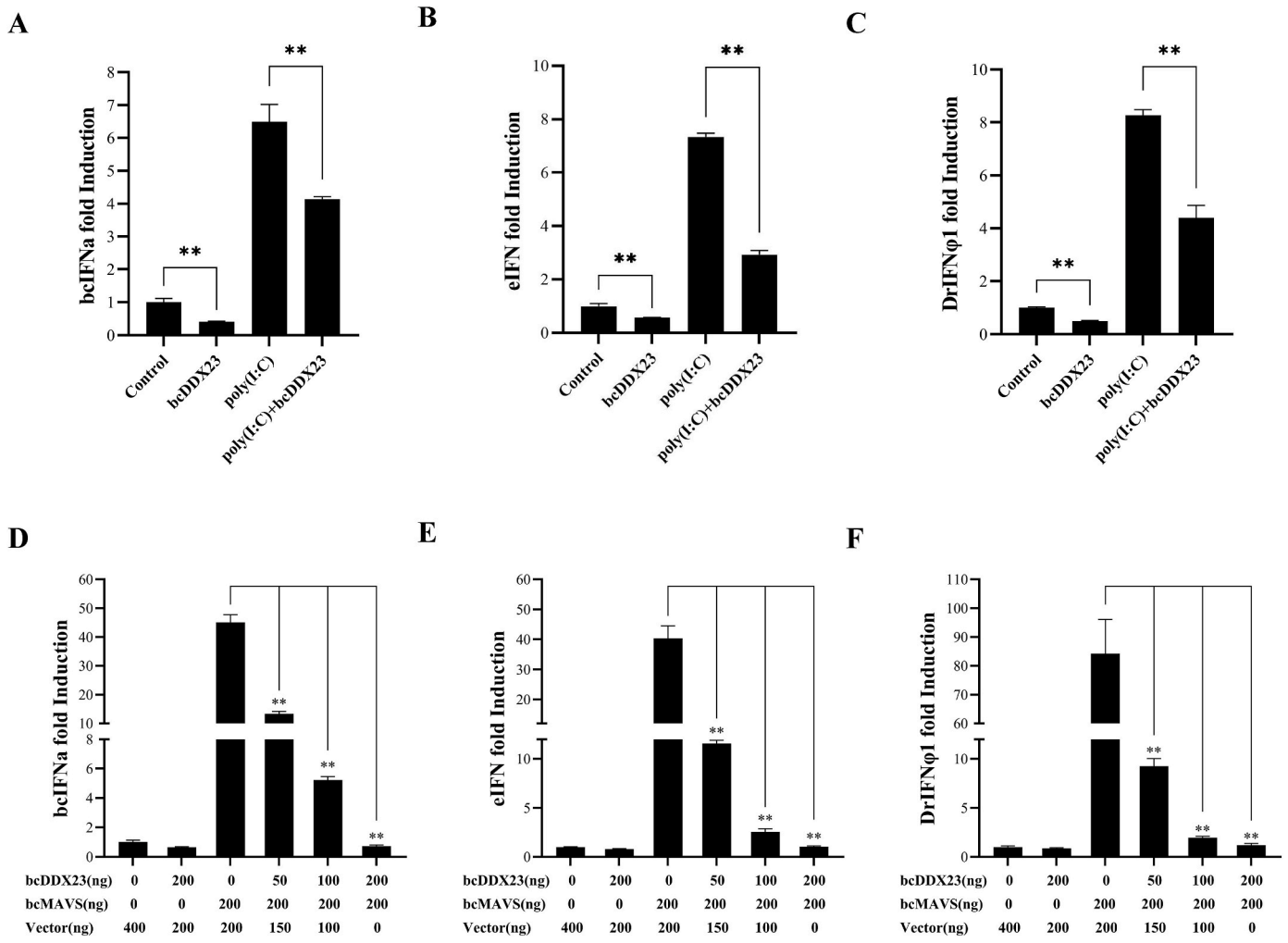

Fig. 6. bcDDX23 inhibits MAVS mediated interferon production.
(**A-C**): The reporter plasmid pRL-TK, Luci-bcIFNa (A)/Luci-eIFNa (B)/Luci-DrIFNφ1 (C) were co-transfected into EPC cells with bcDDX23 or/and poly(I:C). (**D-F**): The reporter plasmid pRL-TK, Luci-bcIFNa (D)/Luci-eIFNa (E)/Luci-DrIFNφ1 (F) were co-transfected into EPC cells with the indicated different doses of plasmids, respectively. The transcription activities of IFN promoters were detected by the luciferase reporter assay. bcDDX23: pcDNA5/FRT/TO/HA-bcDDX23; bcMAVS: pcDNA5/FRT/TO-Flag-bcMAVS, Vector: pcDNA5/FRT/TO. *P < 0.05, **P < 0.01.

3.4. bcDDX23 inhibits MAVS mediated interferon production

According to reporter assay results, over-expressing bcDDX23 in EPC cells could inhibit the transcriptional activity of the bcIFNa, eIFN and DrIFNφ1 promoters. Stimulation by poly (I:C) could enhance the transcriptional activity of the bcIFNa, eIFN and DrIFNφ1 promoters, while over-expressing bcDDX23 significantly inhibited the transcriptional activity of the type I interferon promoter induced by poly (I:C) (Fig. 6A–C). Subsequently, in order to further explore the role of bcDDX23 in the bcMAVS mediated IFN signaling pathway, plasmids expressing bcMAVS or/and bcDDX23 were introduced into EPC cells. The results revealed that bcDDX23 repressed bcMAVS-mediated IFN promoter transcription by a dosage dependent manner (Fig. 6D–F). This suggests that bcDDX23 negatively regulates MAVS/IFN cascade.

3.5. Over-expression of bcDDX23 suppress bcMAVS-mediated antiviral response

The crystal violet staining revealed that over-expressing bcMAVS in EPC cell lines remarkably enhanced cellular resistance to SVCV infection, while co-expression with bcDDX23 markedly reduced the capacity for resistance of cells to SVCV infection (Fig. 7A). Viral titer results showed that bcMAVS markedly inhibited SVCV replication in EPC cells, however its inhibition for SVCV replication was significantly reduced when bcMAVS was co-expressed with bcDDX23 (Fig. 7B). Further study by qPCR assay revealed that the mRNA levels of IFN signaling pathway related genes (*epcIFN*、*epcMX1*、*epcPKR*、*epcIRF7*) mediated by bcMAVS were all reduced to different degrees in EPC cells after SVCV infection (Fig. 7C–F). Meanwhile, the mRNA expression of *SVCV-G*, *N*, *M* and *P* were increased in EPC cells (Fig. 7G). In conclusion, these data indicate that bcDDX23 down-regulates bcMAVS-mediated antiviral response.

3.6. Interfering bcDDX23 expression reinforces antiviral ability in MPK cells

To investigate the role of bcDDX23 in antiviral activity in host cells, shRNA was designed to knockdown bcDDX23 in MPK cells. The decline levels of bcDDX23 in knockdown cells at both protein and gene were examined by IB and qPCR, respectively. The results suggest that shDDX23-1 could slightly reduce exogenous bcDDX23 protein expression level (no statistical difference), while shDDX23-2 reduced about 50% protein expression level of bcDDX23 in HEK293T cells (Fig. 8A–B). The qPCR results showed that over-expression of shDDX23-2 in MPK cells remarkably decreased endogenous bcDDX23 mRNA expression (about 40%) (Fig. 8C). MPK cells transfected with shDDX23-2 or

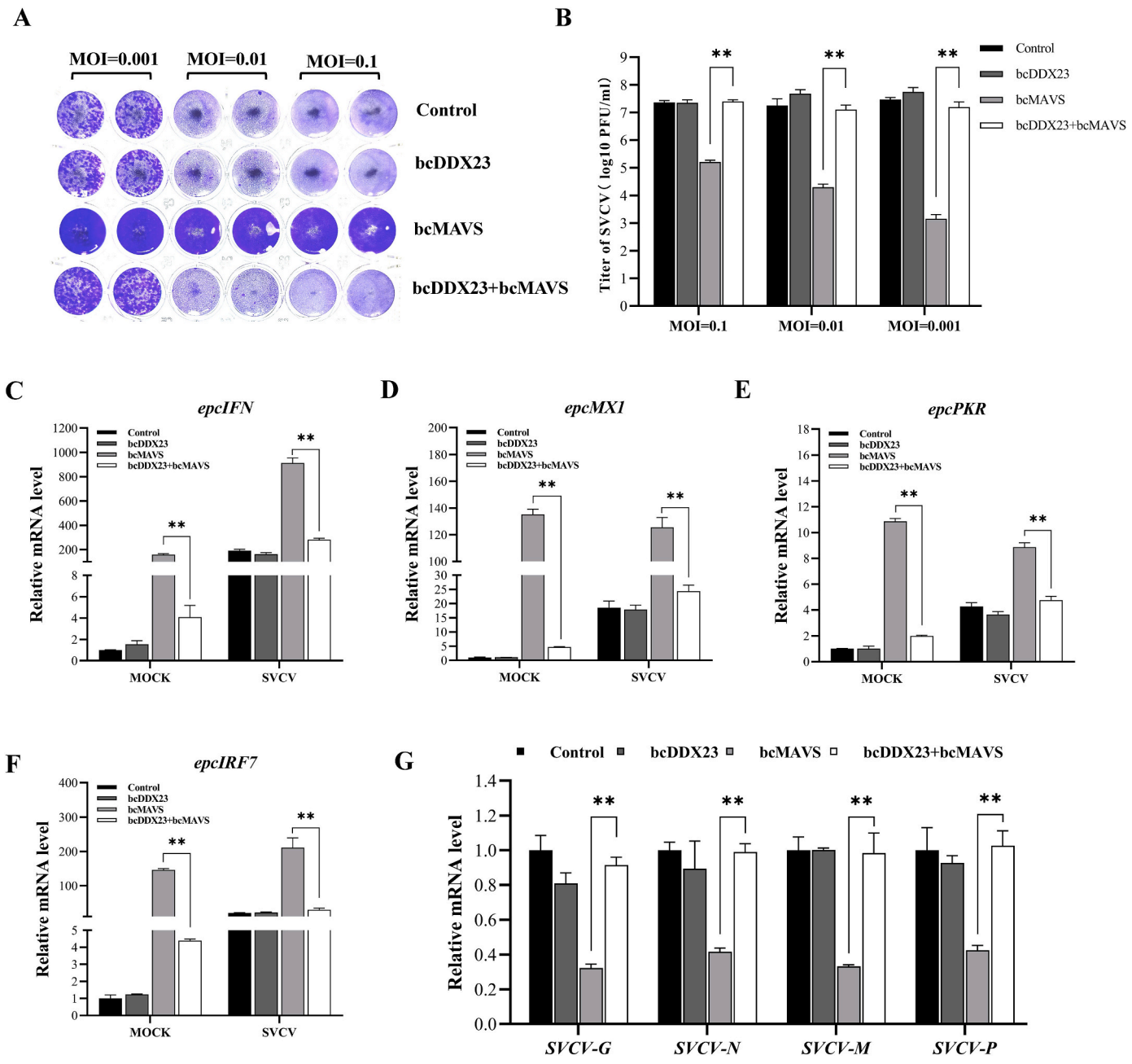

Fig. 7. Over-expression of bcDDX23 suppress bcMAVS-mediated antiviral activity.
(**A-B**): EPC cells in 24-well plate were singly transfected with bcDDX23, bcMAVS or co-transfected with bcDDX23 and bcMAVS. Cells were infected with SVCV for MOI = 0.1, 0.01 and 0.001 respectively. The cell monolayer was stained with crystal violet at 48 h post infection (A). The virus titers in the supernatant media were determined by plaque assay at 24 h post-infection (B). (**C-G**): EPC cells in 6-well plate were singly transfected with bcDDX23, bcMAVS or co-transfected with bcDDX23 and bcMAVS. 24 hpt, cells were infected with or without SVCV for MOI = 0.1 and used for RNA extraction 4 h post virus infection. The mRNA expression levels of *epcIFN* (C), *epcMX1*(D), and *epcPKR* (E), *epcIRF7* (F), *SVCV-G*, *N*, *M* and *P* (G) were examined by qPCR in each group. bcDDX23: pcDNA5/FRT/TO/HA-bcDDX23; bcMAVS: pcDNA5/FRT/TO/Flag-bcMAVS; control: pcDNA5/FRT/TO. *P < 0.05, **P < 0.01. (For interpretation of the references to color in this figure legend, the reader is referred to the Web version of this article.)

scramble shRNA were infected with SVCV with the MOI of 0.01, and plaque test showed that the viral titer in DDX23 knockdown MPK cells was lower than that of the control group (Fig. 8D). The qPCR results showed that the mRNA levels of *SVCV-N*, *M* and *P* were significantly reduced in DDX23 knockdown MPK cells after SVCV infection (Fig. 8E). Corresponding to these, the transcription of *bcIFNa*, *bcMX1*, *bcPKR* and *bcIRF7* were also promoted after knockdown of DDX23 (Fig. 8F–I). In summary, these data together indicate that knocking down bcDDX23 can enhance the host's antiviral capacity, suggesting that bcDDX23 plays a negative role in the host antiviral response.

3.7. *bcDDX23 interacts with bcMAVS*

For more comprehensive understanding of the mechanism by which bcDDX23 inhibits MAVS-mediated antiviral activity, the interaction between bcDDX23 and bcMAVS was detected by co-IP. The results showed that, when bcDDX23 was used as the decoy protein, a specific band representing bcMAVS was detected in the lanes co-transfected with bcDDX23 and bcMAVS. In the meanwhile, when bcMAVS was used as the decoy protein, a specific band representing bcDDX23 was detected in the lanes co-transfected with bcDDX23 and bcMAVS, while no

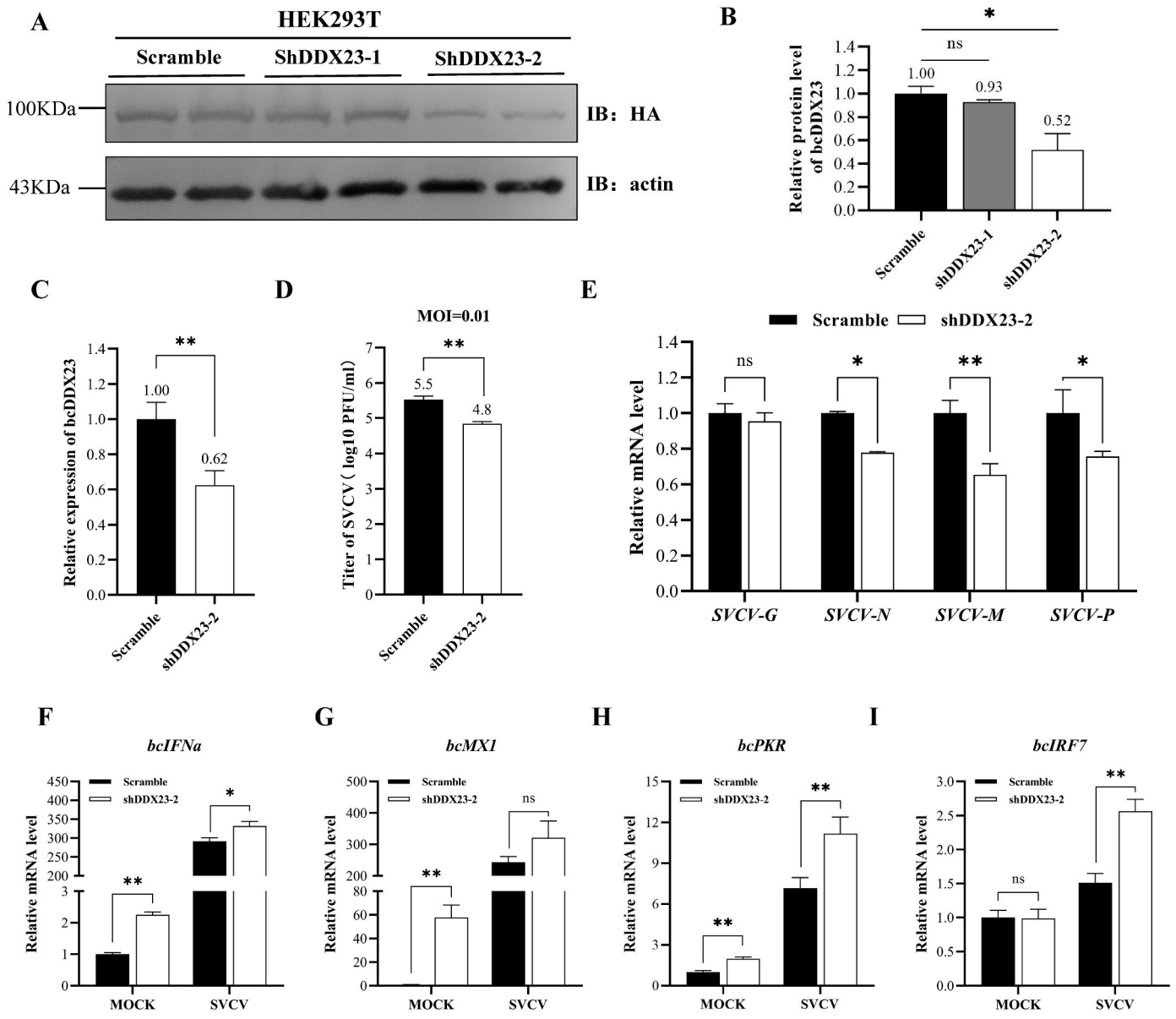

Fig. 8. Interfering bcDDX23 expression reinforces antiviral ability in MPK cells.
(**A**): HEK293T cells in 6-well plates were co-transfected with bcDDX23 (0.5 μg) and shDDX23-1 (2.5 μg) or shDDX23-2 (2.5 μg) or scramble (2.5 μg), respectively, and bcDDX23 expression was detected by IB. (**B**): The bcDDX23 protein expression levels were quantified by imageJ software, and the scramble group was used as 1. (**C**): MPK cells in 6-well plates were transfected with scramble or shDDX23-2, and endogenous mRNA levels of bcDDX23 were detected by qPCR. (**D**): In 24-well plates, MPK cells knocked down with DDX23 were infected with SVCV at MOI = 0.01 and supernatants were collected after 24 h for viral titer assays. (**E-I**): MPK cells were transfected with scramble or shDDX23-2 with or without SVCV infection at an MOI of 0.1, the mRNA expression levels of *SVCV-G*, *N*, *M* and *P* (E), *bcIFNa* (F), *bcMX1* (G), *bcPKR* (H) and *bcIRF7* (I) were detected by qPCR 24 h later. bcDDX23: pcDNA5/FRT/TO/HA-bcDDX23; shDDX23-1:PLKO-shRNA-bcDDX23-1; shDDX23-2: PLKO-shRNA-bcDDX23-2; Scramble: PLKO-shRNA-scramble. ns: no significance, *P < 0.05, **P < 0.01.

corresponding band was found in the control group. These results suggest the bcDDX23 interacts with bcMAVS (Fig. 9A–B).

4. Discussion

DExD/H-box helicase play as either a positive or negative regulator in innate immune signaling cascade and can also act as a direct antiviral effector (Bonaventure and Goujon, 2022). In mammals, DDX3 was able to sense HIV-1 and induce type I interferon production via MAVS (Gringhuis et al., 2017); DDX46 and DDX39A were found to play a negative regulatory role in the antiviral innate response (Shi et al., 2020; Zheng et al., 2017). In a recent comparative immunology study, DDX23 was identified as an evolutionarily conserved dsRNA sensor capable of sensing RNA viruses (Ruan et al., 2019). Although in mammals, DDX23 plays a crucial role in innate immune activation, the role of DDX23 in lower vertebrates is not yet understood (Ruan et al., 2019). In this study, we identified bcDDX23 and explored its function and regulatory mechanism in the antiviral innate immune response.

The activation of innate immunity is vital for host defensing against pathogen invasion, but the regulation of signaling is also indispensable for the prevention of autoimmune diseases. MAVS, as a key adaptor molecule in the RLR/IFN signaling pathway, is tightly regulated to maintain intracellular homeostasis (Liu and Gao, 2018; Wu and Chen, 2014). In mammals, nemo-like kinase (NLK) mediates the phosphorylation of MAVS and leads to its degradation thereby negatively regulating the antiviral signaling pathway. SMAD-specific E3 ubiquitin

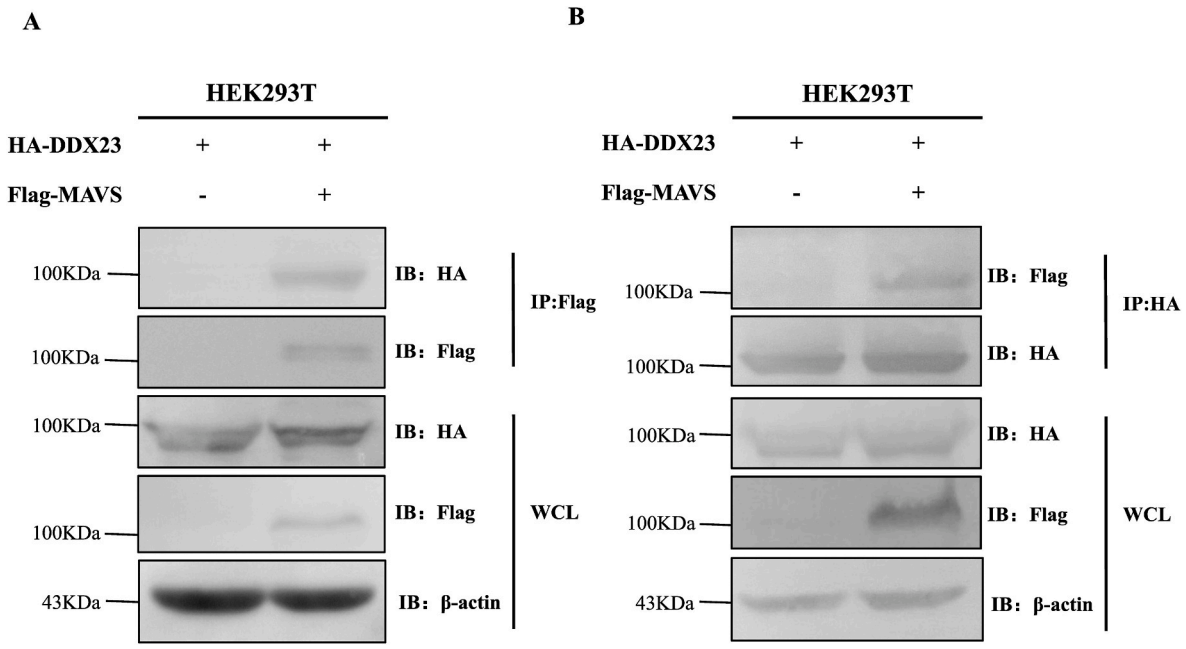

Fig. 9. bcDDX23 interacts with bcMAVS.
(A- B): HEK293T cells in 10 cm dishes were co-transfected with bcDDX23 (5 μg) and bcMAVS (10 μg) or empty vector (10 μg), and after 48 h, cells were harvested and used for immunoprecipitation (IP). The IP was performed using bcDDX23 (A) and bcMAVS (B) as decoy proteins, separately. IP: immunoprecipitation, IB: immunoblotting, WCL: whole cell lysate. bcDDX23:pcDNA5/FRT/TO/HA-bcDDX23; bcMAVS: pcDNA5/FRT/TO/Flag-bcMAVS.

protein ligase 2 (SMURF2) promotes the ubiquitination and degradation of MAVS and thus inhibits the MAVS-mediated antiviral response (Li et al., 2019; Pan et al., 2014). Ever increasing evidence suggests that some members of DExD/H helicases play critical roles in antiviral innate immune responses. Several members of the DExD/H-box helicase, such as DDX3 and DHX9, have also been reported to interact with MAVS. In mammals, DDX3 is able to bind with MAVS and enhance the induction potential of IFNβ induction; and DHX9 has been found to be a MAVS-dependent RNA virus sensor (Oshiumi et al., 2010; Zhang et al., 2011). In our previous studies, we have identified several factors that negatively regulate the MAVS/IFN signaling cascade, such as bcNLRX1, bcNLK and bcRIPK1 (Xiao et al., 2023). In this study, we showed that bcMAVS-mediated antiviral ability was negatively regulated by bcDDX23, which firstly revealed the regulatory role of DDX23 in MAVS mediated antiviral signaling in teleost.

Mammalian DDX23 is composed of N-terminal region, DEXDc domain and HELICc domain, among which N-terminal region can bind poly(I:C) and is essential for downstream signaling, and DEXDc domain is required for MAVS binding (Ruan et al., 2019). The structure of bcDDX23 is very similar to that of mammalian DDX23, which also consists of the above three structural domains. However, there is a large difference in homology between the two in the N-terminal region. Human DDX23 has been reported to be able to sense the RNA virus and activate the antiviral signaling of host by interacting with TRIF or MAVS (Ruan et al., 2019). In this study, our results showed that bcDDX23 interacted with bcMAVS and suppressed MAVS-mediated IFN production, thereby attenuating the host's antiviral activity, which is different from its mammalian counterpart. We speculate that the sequence and structure differences at the N-terminal region might account for the functional difference between bcDDX23 and human DDX23. However, the specific mechanism still needs further investigate. This study not only extends our understanding of the function of DDX23 in antiviral innate immunity from higher vertebrates to lower vertebrates, but also further enriches the regulatory mechanisms of innate immunity in fish.

Most helicases are localized in the nucleus, and their translocation are associated with viral replication in host cells. Some recent studies on the role of helicases in antiviral responses have revealed that porcine reproductive and respiratory syndrome virus (PRRSV) infection enhances the expression of DDX21 and promotes its nuclear to cytoplasmic translocation; the chikungunya virus (CHIKV) infection increases the amount of DDX56 in the cytoplasm; the DDX23 translocates from the nucleus to the cytoplasm after VSV or FMDV stimulation (Abdullah et al., 2020; Li et al., 2022; Ruan et al., 2019; Taschuk et al., 2020). In the current investigation we analyzed the subcellular localization of bcDDX23 and found that its distribution in the cytoplasm increased after SVCV stimulation, which was consistent with the previous studies. Together, the above results suggest that DDX23 is widely involved in various types of RNA virus-host interaction and its mechanism of translocation is cross-species.

In conclusion, the current studies suggest that bcDDX23 plays a negative regulatory role in antiviral innate immune activation. Different from its mammalian counterpart, DDX23 does not act as a positive regulator in black carp, but rather inhibits the MAVS-mediated RLR/IFN signaling cascade response by interacting with MAVS. Together, these findings suggest that the innate immune regulation mechanism of black carp has its uniqueness and investigation on the antiviral mechanism by innate immune in black carp may reveal some novel immune regulatory mechanisms and expand the understanding of the whole vertebrate (including human) innate immune system.

Data availability

Data will be made available on request.

Acknowledgments

This work was supported the National Natural Science Foundation of China (U21A20268, U22A20535, 32173010, 32002415), the Modern Agricultural Industry Program of Hunan Province, Hunan Provincial education Department (20A317), Hunan Provincial Science and Technology Department (2023JJ10010028, 2022JJ30383), Training Program for Excellent Young Innovators of Changsha (kq2206023).

References

Abdullah, S.W., Han, S., Wu, J., Zhang, Y., Bai, M., Jin, Y., Zhi, X., Guan, J., Sun, S., Guo, H., 2020. The DDX23 negatively regulates translation and replication of foot-and-mouth disease virus and is degraded by 3C proteinase. Viruses 12, 1348.

Akira, S., Uematsu, S., Takeuchi, O., 2006. Pathogen recognition and innate immunity. Cell 124, 783–801.

Ashraf, U., Lu, Y., Lin, L., Yuan, J., Wang, M., Liu, X., 2016. Spring viraemia of carp virus: recent advances. J. Gen. Virol. 97, 1037–1051.

Bonaventure, B., Goujon, C., 2022. DExH/D-box helicases at the frontline of intrinsic and innate immunity against viral infections. J. Gen. Virol. 103.

Cao, Y., Chen, Z., Huang, J., Wu, H., Zou, J., Feng, H., 2021. Black carp TUFM collaborates with NLRX1 to inhibit MAVS-mediated antiviral signaling pathway. Dev. Comp. Immunol. 122, 104134.

Carty, M., Guy, C., Bowie, A.G., 2021. Detection of viral infections by innate immunity. Biochem. Pharmacol. 183, 114316.

Chen, J.Y.-F., Stands, L., Staley, J.P., Jackups, R.R., Latus, L.J., Chang, T.-H., 2001. Specific alterations of U1-C protein or U1 small nuclear RNA can eliminate the requirement of Prp28p, an essential DEAD box splicing factor. Mol. Cell 7, 227–232.

Chen, Z., Cao, Y., Huang, J., Tan, Y., Wei, J., Xiao, J., Zou, J., Feng, H., 2021. NLK suppresses MAVS-mediated signaling in black carp antiviral innate immunity. Dev. Comp. Immunol. 122, 104105.

Fang, R., Jiang, Q., Zhou, X., Wang, C., Guan, Y., Tao, J., Xi, J., Feng, J.-M., Jiang, Z., 2017. MAVS activates TBK1 and IKKε through TRAFs in NEMO dependent and independent manner. PLoS Pathog. 13, e1006720.

Funabiki, M., Kato, H., Miyachi, Y., Toki, H., Motegi, H., Inoue, M., Minowa, O., Yoshida, A., Deguchi, K., Sato, H., Ito, S., Shiroishi, T., Takeyasu, K., Noda, T., Fujita, T., 2014. Autoimmune disorders associated with gain of function of the intracellular sensor MDA5. Immunity 40, 199–212.

Gringhuis, S.I., Hertoghs, N., Kaptein, T.M., Zijlstra-Willems, E.M., Sarrami-Forooshani, R., Sprokholt, J.K., van Teijlingen, N.H., Kootstra, N.A., Booiman, T., van Dort, K.A., Ribeiro, C.M.S., Drewniak, A., Geijtenbeek, T.B.H., 2017. HIV-1 blocks the signaling adaptor MAVS to evade antiviral host defense after sensing of abortive HIV-1 RNA by the host helicase DDX3. Nat. Immunol. 18, 225–235.

Konishi, T., Uodome, N., Sugimoto, A., 2008. The *Caenorhabditis elegans* DDX-23, a homolog of yeast splicing factor PRP28, is required for the sperm-oocyte switch and differentiation of various cell types. Dev. Dynam. 237, 2367–2377.

Krishnan, V., Zeichner, S.L., 2004. Alterations in the expression of DEAD-box and other RNA binding proteins during HIV-1 replication. Retrovirology 1, 42.

Li, J., Wang, D., Fang, P., Pang, Y., Zhou, Y., Fang, L., Xiao, S., 2022. DEAD-box RNA helicase 21 (DDX21) positively regulates the replication of porcine reproductive and respiratory syndrome virus via multiple mechanisms. Viruses 14, 467.

Li, S.-Z., Shu, Q.-P., Song, Y., Zhang, H.-H., Liu, Y., Jin, B.-X., Liuyu, T.-Z., Li, C., Huang, X.-C., Du, R.-L., Song, W., Zhong, B., Zhang, X.-D., 2019. Phosphorylation of MAVS/VISA by Nemo-like kinase (NLK) for degradation regulates the antiviral innate immune response. Nat. Commun. 10, 3233.

Liu, B., Gao, C., 2018. Regulation of MAVS activation through post-translational modifications. Curr. Opin. Immunol. 50, 75–81.

Liu, Y., Xiao, J., Qiao, G., Wang, Q., Yang, X., Xu, X., Li, J., Zhang, J., Chang, M., Feng, H., 2022. DDX19 inhibits RLR/IRF3 mediated type I interferon signaling of black carp Mylopharyngodon piceus by restricting IRF3 from entering nucleus. Aquaculture 553, 738087.

Oshiumi, H., Sakai, K., Matsumoto, M., Seya, T., 2010. DEAD/H BOX 3 (DDX3) helicase binds the RIG-I adaptor IPS-1 to up-regulate IFN-β-inducing potential. Eur. J. Immunol. 40, 940–948.

Pan, Y., Li, R., Meng, J.-L., Mao, H.-T., Zhang, Y., Zhang, J., 2014. Smurf2 negatively modulates RIG-I–dependent antiviral response by targeting VISA/MAVS for ubiquitination and degradation. J. Immunol. 192, 4758–4764.

Ramos, H.J., Gale, M., 2011. RIG-I like receptors and their signaling crosstalk in the regulation of antiviral immunity. Curr. Opin. Virol. 1, 167–176.

Rehwinkel, J., Gack, M.U., 2020. RIG-I-like receptors: their regulation and roles in RNA sensing. Nat. Rev. Immunol. 20, 537–551.

Robert, X., Gouet, P., 2014. Deciphering key features in protein structures with the new ENDscript server. Nucleic Acids Res. 42, W320–W324.

Rönnblom, L., Eloranta, M.-L., 2013. The interferon signature in autoimmune diseases. Curr. Opin. Rheumatol. 25, 248–253.

Ruan, J., Cao, Y., Ling, T., Li, P., Wu, S., Peng, D., Wang, Y., Jia, X., Chen, S., Xu, A., Yuan, S., 2019. DDX23, an evolutionary conserved dsRNA sensor, participates in innate antiviral responses by pairing with TRIF or MAVS. Front. Immunol. 10, 2202.

Shi, P., Guo, Y., Su, Y., Zhu, M., Fu, Y., Chi, H., Wu, J., Huang, J., 2020. SUMOylation of DDX39A alters binding and export of antiviral transcripts to control innate immunity. J. Immunol. 205, 168–180.

Takeuchi, O., Akira, S., 2010. Pattern recognition receptors and inflammation. Cell 140, 805–820.

Taschuk, F., Tapescu, I., Moy, R.H., Cherry, S., 2020. DDX56 binds to chikungunya virus RNA to control infection. mBio 11, e02623, 20.

Wang, C., Li, J., Yang, X., Wang, Q., Zhong, H., Liu, Y., Yan, W., He, Y., Deng, Z., Xiao, J., Feng, H., 2021. Black carp IKKε collaborates with IRF3 in the antiviral signaling. Fish Shellfish Immunol. 118, 160–168.

Wu, J., Chen, Z.J., 2014. Innate immune sensing and signaling of cytosolic nucleic acids. Annu. Rev. Immunol. 32, 461–488.

Xiao, J., Zhong, H., Feng, H., 2023. Post-translational modifications and regulations of RLR signaling molecules in cytokines-mediated response in fish. Dev. Comp. Immunol. 141, 104631.

Xue, T., Wang, Y.Z., Pan, Q.H., Wang, Q., Yuan, J.F., Chen, T.S., 2018. Establishment of a cell line from the kidney of black carp and its susceptibility to spring viremia of carp virus. J. Fish. Dis. 41, 365–374.

Yang, X., Ai, Y., Chen, L., Wang, C., Liu, J., Zhang, J., Li, J., Wu, H., Xiao, J., Chang, M., Feng, H., 2023. PRKX down-regulates TAK1/IRF7 signaling in the antiviral innate immunity of black carp Mylopharyngodon piceus. Front. Immunol. 13, 999219.

Zhang, Z., Yuan, B., Lu, N., Facchinetti, V., Liu, Y.-J., 2011. DHX9 pairs with IPS-1 to sense double-stranded RNA in myeloid dendritic cells. J. Immunol. 187, 4501–4508.

Zheng, Q., Hou, J., Zhou, Y., Li, Z., Cao, X., 2017. The RNA helicase DDX46 inhibits innate immunity by entrapping m6A-demethylated antiviral transcripts in the nucleus. Nat. Immunol. 18, 1094–1103.

Zhu, L., Nie, L., Zhu, G., Xiang, L., Shao, J., 2013. Advances in research of fish immune-relevant genes: a comparative overview of innate and adaptive immunity in teleosts. Dev. Comp. Immunol. 39, 39–62.